

Point and Ask: Incorporating Pointing into Visual Question Answering

Arjun Mani, Will Hinthorn*, Nobline Yoo, Olga Russakovsky
Princeton University

{arjuns, olgarus}@cs.princeton.edu

Abstract

Visual Question Answering (VQA) has become one of the key benchmarks of visual recognition progress. Multiple VQA extensions have been explored to better simulate real-world settings: different question formulations, changing training and test distributions, conversational consistency in dialogues, and explanation-based answering. In this work, we further expand this space by considering visual questions that include a spatial point of reference. Pointing is a nearly universal gesture among humans, and real-world VQA is likely to involve a gesture towards the target region.

Concretely, we (1) introduce and motivate point-input questions as an extension of VQA, (2) define three novel classes of questions within this space, and (3) for each class, introduce both a benchmark dataset and a series of baseline models to handle its unique challenges. There are two key distinctions from prior work. First, we explicitly design the benchmarks to require the point input, i.e., we ensure that the visual question cannot be answered accurately without the spatial reference. Second, we explicitly explore the more realistic point spatial input rather than the standard but unnatural bounding box input. Through our exploration we uncover and address several visual recognition challenges, including the ability to infer human intent, reason both locally and globally about the image, and effectively combine visual, language and spatial inputs. Code is available at: github.com/princetonvisualai/pointingqa.

1. Introduction

Visual Question Answering (VQA) has emerged as a popular and challenging task in computer vision [3, 13, 34, 16, 8, 7]. When the task was first introduced, the challenge of answering a natural language question about an image was already a significant leap beyond more conventional tasks such as object recognition. Since then, questions in VQA benchmarks have been increasingly growing in complexity: for example, “Are there any cups to the left of the



What color is *this* dog? What is *this*? Is another dog *this* breed?
Figure 1. Three types of visual questions requiring a point (green).

tray on top of the table?” is an example question from the recent GQA [16] benchmark. Such questions effectively test the ability of VQA agents to parse very complex sentences, but arguably are becoming less realistic. In a real-world setting, it’s unlikely that a human would use the phrase “to the left of the tray on top of the table.” It’s far more likely that they would instead ask “Are there any cups over there” and point to the left of the tray. In fact, human psychology literature shows that pointing to interesting objects or situations is one of the first ways by which babies communicate intention [25, 22]. Understanding pointing as part of a visually grounded dialog with humans would naturally be a key ability of real-world AI systems.

We thus propose to expand the space of VQA by considering visual questions that further include a spatial point of reference for context. Prior works have used visual grounding to expand the question space of VQA: e.g., Visual7W [34] introduced “which” question with image regions as candidate answers; Visual Genome [19] contains questions that are associated with particular regions in the image; GQA [16] leverages the grounded scene graph in its question construction process. There are two key distinctions of our proposal from this line of work. First, we explicitly design the benchmarks to *require* the point input, i.e., we ensure that the visual question cannot be answered accurately without the spatial reference. Second, we explore the more realistic *point* spatial input rather than the standard but unnatural bounding box used in [34, 19, 16].

We define three novel types of visual questions using a point for contextual reference as shown in Figure 1: (1) **Local-QA**, where only the local region around the point is relevant to the question, e.g., “What color is *this* shirt?” where *this* is specified by a pixel in the image; (2)

*WH is currently at Microsoft. Work was conducted while he was an undergraduate student at Princeton University.

Intent-QA, expanding on Local-QA by requiring a more advanced form of contextual reasoning through questions like “what is *this*?”; and (3) **LookTwice-QA**, which requires a global understanding of the image, e.g., “is another shirt *this* color?” Within each question type, we introduce both benchmark datasets and baseline models. Local-QA and LookTwice-QA datasets are constructed from Visual Genome annotations [19] and contain 57,628 questions across 18,830 images and 57,405 questions across 34,676 images, respectively. For Intent-QA, where the model must reason about the human intent of the reference point, we crowdsource a dataset of 49,623 human annotated points across 8,204 images and 15 objects.

Concretely, we (1) introduce and motivate point-input questions as an extension of VQA, (2) define three novel types of questions within this space, and (3) for each type, introduce both a dataset and appropriate model designs to handle the unique challenges. With empirical evaluation we demonstrate that (a) it is possible to both consistently annotate as well as train a model to reliably predict the intent of a single point in Intent-QA, and (b) our point-aware models significantly outperform existing VQA systems and multiple baselines on the new tasks.

2. Related Work

Spatial Grounding in VQA. Visual grounding has become a central idea in the VQA community [34, 13, 1, 16]. It is increasingly seen as important that VQA models localize the object being asked about to answer a visual question. This idea has influenced the development of several datasets, including Visual7W [34] and GQA [16]. In these datasets, bounding boxes are provided for each object mentioned in the question or answer. To encourage grounding and counteract language priors, [13] introduced the VQA 2.0 Dataset in 2017, which consists of complementary images for each question. [1] further introduce the VQA-CP dataset, where priors differ in training and test splits. All these works indicate the importance of visual grounding for the VQA task.

A few works have used visual grounding to expand the question space of VQA. The authors of Visual7W introduce a *pointing QA* task, involving a ‘which’ question and image regions as candidate answers [34]. They use their manually collected object-level groundings to construct such questions. A number of works have also explored grounding in the context of embodied question answering, which requires an agent to explore an environment to answer a visual question [7, 12]. Other grounding-based questions include region-based QAs in Visual Genome [19], where the question is associated with a particular region of the image. However, it is not necessary for answering the question that the region be provided: we sampled 100 questions randomly and only 17% actually required the region to pro-

duce the correct answer. To our knowledge, we are the first to introduce a benchmark where a spatial grounding signal is explicitly required to answer a question.

The importance of visual grounding has also influenced the development of VQA models. In particular, most state-of-the-art VQA models have an attention mechanism on the image [2, 32, 31]. The relative success of these models indicates the importance of successful visual grounding in the VQA task. Several works include pixel-wise prediction as a primary or auxiliary task of the VQA model. [33] mine ground-truth attention maps from Visual Genome and include attention prediction explicitly as an auxiliary task of the model. Other works output a visual justification for the answer as a heatmap [27] or a semantic segmentation of the visual entities relevant to the question [11]. However, the challenge of actually accepting a spatial grounding input into VQA models has not been previously explored.

Point input. Despite being ubiquitous for humans, pointing as a way of communicating intention has been underexplored in computer vision. Studies in the robotics [15, 30, 28] or human-computer interaction [23] communities have largely been limited to simple, constrained environments. In vision, pointing has been used as a form of cost-effective supervision [4, 17, 26, 5] but never examined in depth beyond cost-accuracy tradeoffs. The use of pointing as a communicative gesture in humans [25, 22] motivates deeper study in a computer vision context.

3. Tasks

To study the problem of spatial disambiguation in Visual Question Answering (VQA) we introduce three tasks exploring different aspects and challenges of this question space. In all three tasks the input is an image and a single pixel in the image corresponding to the spatial grounding. The target output is a multiple choice answer.

Local-QA. The first type of questions involves queries about the attributes of a particular object (e.g. “What color is *this* car?”). These questions are local, i.e., a local region around the point is completely sufficient to answer the question. Moreover, it is unnecessary to infer the intended object of reference from the point alone; this is provided by the question. The primary challenge of Local-QA is for the model to accept a point input, which we study in detail. An important challenge is to vary attention around the point depending on the question (consider “What color is this shirt?” and “What action is this person doing?”).

Intent-QA. We next want to extend Local-QA by requiring the model to explicitly reason about the spatial extent of the point: for example, by asking “what shape is *this*?” without having to specify what *this* is referring to beyond the single point. Such questions often appear in real-world settings, where the recipient of the question is expected to infer the

intended reference from a pointing gesture. To explicitly test the ability of the model to infer the intended reference, independent of its ability to answer Local-QA questions, we limit Intent-QA to the simple but still surprisingly challenging question “what is *this*?”. To further scope this study, we focus on learning whether a human intends to refer to the whole object versus a specific part of the object: consider a point on torso vs. on hand, or the point on the ear of the dog vs on a dog’s body in Figure 1. We assume that a human pointing to a pixel is referring to either the object or the object part occupying that pixel. This task can be framed either as a VQA or segmentation task and we explore both approaches. Efficiently collecting this dataset poses a number of crowdsourcing challenges.

LookTwice-QA. In the second extension of Local-QA we consider questions that require spatial reasoning beyond the local image region. A natural example is counting questions such as “How many of *this* animal are there?”, where the model must identify the relevant object around the point and then use this information to attend to the entire image. These questions require the model to “look twice,” first at the point and then at the entire image. The challenge is to perform this two-step compositional reasoning.

4. Datasets

We construct a dataset for each of the new tasks in Sec. 3. We use existing annotations from Visual Genome [19] and PASCAL VOC [9, 6] whenever possible, and supplement with crowdsourced annotations as needed. For all datasets, we ensure by construction that the point input is required: every question we include is ambiguous (has multiple correct answers) in the absence of the reference point.

4.1. Local-QA 1.0 dataset

The Local-QA 1.0 dataset contains questions that require reasoning over a local image region, with the point input disambiguating the correct region. We use three templates:

1. What color is *this* [object class]?
2. What shape is *this* [object class]?
3. What action is *this* [object class] doing?

We generate the dataset from Visual Genome [19], which consists of 108,249 images with each image annotated on average with 35 objects, 26 object attributes, and 21 pairwise relationships between the objects.

Attribute selection. We select the 100 most common attributes from Visual Genome (e.g. red, round, small), which account for 70.1% of annotations. We manually group these attributes into four general categories: color, shape, action, and size. We only use the first three categories, as size is a relative rather than an absolute property of the object.

Question Generation. On every image in Visual Genome, we search for examples that satisfy the constraints of Local-

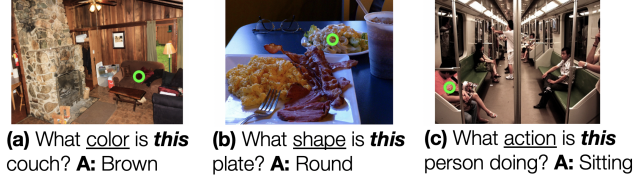


Figure 2. Examples of questions in the Local-QA Dataset across color, shape, and action. Point is indicated in green.

QA. Concretely, we examine pairs of bounding boxes b_i, b_j annotated with corresponding object classes o_i, o_j and the sets of attributes A_i, A_j . If $o_i = o_j$, so the object classes are the same, we then look for a pair of attributes $a_i \in A_i, a_j \in A_j$ such that $a_i \neq a_j$ and a_i, a_j are of the same category (color, shape or action). We construct a question q of the form “What C is this O ?”, where C is the attribute category and $O = o_j = o_k$ the object class. We then add two examples into our dataset: (1) question q , point to the center of the bounding box b_i , and answer a_i , and (2) question q , point to center of b_j and answer a_j .

We performed several optimizations to ensure quality. Instances where $\text{IoU}(b_i, b_j) \geq t$ were filtered out (we set $t = 0.2$ to maximize precision). Any object with more than one attribute in the same category was excluded (e.g., a striped shirt annotated as both “red” and “white”) to avoid confusion. Attributes that are visually similar or identical (e.g., ‘grey’ and ‘gray’, ‘blonde’ and ‘yellow’) were collapsed into a single attribute to reduce noise.

Statistics. The final dataset consists of 57,628 questions across 18,380 images, with 20 unique answers. Due to the high representation of color attributes in Visual Genome, 97.2% of questions are about color, with the remaining being about shape or action. Although biased in this way, the relative simplicity of color questions allows us to focus on the challenge of incorporating a point input. Although most questions have exactly two unique answers without a disambiguating point, 11.9% of questions would have greater than two unique answers. Fig. 2 shows example questions in the dataset. These examples illustrate the challenges of answering point-input questions, especially when the point can be placed on a non-relevant part of an object (Fig 2a, Fig 2c) or on another smaller, occluding object (Fig 2b).

The images are randomly divided into (1) *train*, 70%, with 40,409 questions across 12,867 images; (2) *val*, 10%, with 5,724 questions across 1,838 images; (3) *test-dev*, 10%, with 5,673 questions across 1,838 images, and (4) *test-final*, 10%, at 5,910 questions across 1,837 images. We recommend using *val* for hyperparameter tuning, *test-dev* for ablation studies, and *test-final* to report results.

4.2. Intent-QA 1.0 dataset

Our second dataset benchmarks the model’s ability to infer intent and produce the most appropriate response to a

question “What is *this*?” about a point in the image. To do so, the model must be able to disambiguate between multiple choices, all of which are technically correct descriptions of the point, and decide which one is the most likely. For instance, pointing at a cat’s tail may refer to the tail specifically, while a point on its torso could refer to the cat as a whole. The correct response would depend on the location of the point, as well as the cat’s orientation and surrounding visual context.

Such annotations of intent do not currently exist to the best of our knowledge, so we crowdsource the dataset. To scope the study, we restrict the answers to take one of two forms: (1) object of class C or (2) part of the object of class C , for a pre-defined set of classes.

Point Generation. We leverage existing pixel-level segmentation masks of object and parts in PASCAL VOC [9, 6, 24] to generate a promising set of points to annotate. Using the semantic object and part masks, we compute the medial axis skeleton for each mask and draw points following a distribution modeling humans pointing to objects [10]. To create a balanced dataset, for each semantic object category, we present annotators with an even ratio of points generated from the whole object masks and constituent part masks.

Crowdsourced annotation. For every point we already know the corresponding object class by construction and only need the annotators to determine the likely intent. Taking the cat’s tail example from above, we ask annotators to select whether a human pointing to this pixel is most likely referring to: (1) “the cat,” (2) “the cat’s tail” (3) “impossible to tell” or (4) “neither one.”. This simplified interface allowed us to collect 49,623 manually annotated points corresponding to 15 object classes and their parts, for total 30 classes. Each point is labeled by at least three annotators.

Statistics. Impressively, 67% of points have perfect inter-annotator agreement, and the average human annotator accuracy (evaluated against the other annotators) is 86.9%. This indicates that despite the possibility of the intended reference being ambiguous, the task itself is doable by humans while presenting significant new challenges to VQA systems. The dataset is well-balanced with 57% of the points referring to an object part. Example annotations are shown in Fig. 3. For the purposes of training, we label points as their majority label and remove those marked neither/impossible or where no majority opinion exists, for a total of 48,143 points. The images are randomly divided into (1) *train*, 70%, with 33,864 points across 5,703 images; (2) *val*, 10% with 4,445 points across 814 images; (3) *test-dev*, 10%, with 5,092 points across 814 images, and (4) *test-final*, 10%, at 4,742 points across 814 images.



Figure 3. Examples of annotations in the Intent-QA dataset: (Left) Dog, Part; (Middle) Horse, Object; (Right) Person, Ambiguous.

4.3. LookTwice-QA 1.0 dataset

Finally, we construct the LookTwice-QA dataset where the model needs to first understand the local region around the point and then use this local information to reason about the rest of the image. A natural example is counting questions. A standard VQA counting question (e.g. “How many trucks are there?”) can be rephrased to include a point input as (1) “How many of *these* vehicles are there?”, or more generally (2) “How many of *these* are there?”. Such questions require both extracting appropriate local features as well as reasoning globally to count the instances.

We construct the dataset leveraging human-written counting questions in Visual Genome [19]. We augment these using questions automatically generated from Visual Genome object annotations; however, these are prone to under-counting when the object annotation recall is low and are thus only utilized during training.

Question Generation. There are 99,860 human-written counting questions in Visual Genome. For each question, we extract the subject of the question (an object class, e.g., “truck”) and attempt to match it to an annotated object in the image. If multiple objects exist, one is chosen at random; if none exist, the question is removed. From this filtered question set, questions about object classes appearing less than 100 times total are further removed. The remaining set of object classes are manually grouped into three super-categories: beings (people and animals), vehicles (ex. cars, planes), and objects (ex. laptops, umbrellas). From each question of the form e.g., “How many [object class] are there?” we generate two new questions by replacing the “[object class]” either with (1) “these [supercategory]” or (2) just “these.” We disambiguate the reference through the point input, simulated as the center of the object bounding box. The answer remains the same; we thus train the model to locally infer the basic object category from the point.

Counteracting priors. Our goal is to construct questions that *require* the point input and cannot be answered without it. Thus, we enforce that for each image I in the evaluation set, there are at least two questions q_i, q_j such that $o_i \neq o_j$ (different objects), and $a_i \neq a_j$ (different answers).

The remaining generated questions are added to the training set. To prevent priors in the training set, for each question q_i we use Visual Genome object annotations to generate a question q_j with $o_i \neq o_j$ and $a_i \neq a_j$. Ob-



Figure 4. Example entries in the LookTwice-QA Dataset. Point is shown in green, and the supercategory is underlined.

ject counts are generated from the IoU-filtered object annotations in the image and may be imperfect due to undercounting (thus not used during evaluation). The original question is constructed as “How many o_i are there?”, with the object class in its plural form for readability, and then converted into two generic question types as above.

Statistics. The LookTwice-QA dataset contains 57,405 questions across 34,676 images, including (1) *train* with 37,981 human-written and 14,713 automatically-generated questions across 32,925 images, (2) *val* with 997 human-written questions across 380 images, and (3) *test* with 3,714 human-written questions across 1,371 images.

The answer distribution is reasonably balanced: the answers “1” and “2” appear with 35.4% and 33.7% frequency respectively in the test set; other questions have answer “3” or greater. The most common objects in the dataset are people (29.7%), cars (3.1%), and signs (2.9%). Due to the high representation of people, the most common super-category is beings (48.9%), followed by objects (36.7%) and vehicles (14.3%). Given only the object name, a model can achieve an accuracy of at most 42.1%, indicating that visual reasoning is necessary. Example questions are shown in Fig. 4.

5. Models

We modify standard VQA models to accept a point input. Concretely, we introduce and analyze four models tackling the different challenges of our new tasks: (1) **Local-QA-model** for focusing state-of-the-art region-based VQA systems [2, 32, 31] around a point input, (2) **Local-QA-grid-model** for adapting the new grid-feature-based VQA system [18] to the point input, (3) **Local-Segm-model**, a variation of a semantic segmentation model that can be used for the Intent-QA task, and (4) **Global-QA-model**, an adaptation of the Local-QA-model for the LookTwice-QA questions requiring global reasoning.

Local-QA-model. The Local-QA-model incorporates the point input (x, y) into the state-of-the-art VQA models [2, 32, 31]. We first begin by summarizing these models.

Background. Standard VQA systems [2, 32, 31] represent the image using a set of bounding box proposals from an object detection model, typically Faster-RCNN [29]. Concretely: (a) an object class-agnostic Region Proposal Network extracts a set of candidate regions along with their

“objectness” scores, (b) non-max suppression is performed to remove similar boxes, and (c) the top remaining N regions are processed by an `ROIPOOL` operation and additional network layers to generate a set of visual features $\mathbf{v}_1 \dots \mathbf{v}_N, \mathbf{v}_i \in \mathbb{R}^D$. In step (d), the question is encoded by a recurrent model into $\mathbf{q} \in \mathbb{R}^M$. Then: (e) \mathbf{q} is combined with $\mathbf{v}_1 \dots \mathbf{v}_N$ to compute a normalized attention vector $\mathbf{a} \in \mathbb{R}^N$ over the N region proposals, (f) the probabilistic attention \mathbf{a} is used to compute a weighted average of the region features and obtain the image representation $\mathbf{v} \in \mathbb{R}^D$, and (g) \mathbf{q} and \mathbf{v} are projected to a common vector space, combined via element-wise multiplication followed by fully-connected layers and a softmax activation to predict over the answer distribution. Steps (a)-(c) use a pre-trained detection model, while (d)-(g) are trained.

Modifications. We choose the simplest way of incorporating the point input into the system above: in step (a) above, we remove all candidate regions that do not contain the point (x, y) . The rest of the pipeline is unchanged, apart from zero-padding to N regions if necessary (we use $N = 100$, as is standard). In Sec. 6 we investigate a number of alternatives (e.g., using the \mathbf{v}_i with the highest objectness score of all regions containing the point as the image representation \mathbf{v}) but found them inferior to this approach. Our approach produces the effect of a pointing gesture by restricting the view of the model to objects around the point. It has the additional advantage of allowing us to analyze the learned attention around the point, yielding insights into the behavior of the Local-QA-model.

Local-QA-grid-model. An alternative to region-based features is the newly-proposed grid-based system. Jiang et al. [18] demonstrated that grid features extracted directly from the convolutional layers of a Faster-RCNN (modified with 1×1 `ROIPOOL` during training) can similarly yield strong performance on VQA; concretely, they replace steps (a-c) above with visual features $\mathbf{v}_{ij}, i \in [1, W], j \in [1, H]$ for downsampled image of resolution $W \times H$. In our Local-QA-grid-model we incorporate the point input (x, y) by setting the full-image representation $\mathbf{v} = \mathbf{v}_{ij}$ for ij corresponding to the grid position closest to (x, y) after downsampling. As in the Local-QA-model, we empirically evaluate several alternatives in Sec. 6 that learn attention over the grid features contained within some downsampled bounding box (e.g., highest-scoring region proposal). However, we find our method to be most effective.

Local-Segm-model. The Local-QA-model and Local-QA-grid-model can work on both Local-QA and Intent-QA benchmarks since both evaluate the ability of a system to reason about a local image region. However, Intent-QA has an additional interesting property that depending on the VQA formulation, the asked question can actually be the same across all reference points (e.g. “what is *this* referring to?”) and thus can be also answered by a semantic

segmentation model. We use a Fully Convolutional Network (FCN) [21] with a $2C + 1$ -dimensional output for every pixel in the image: C is the number of object classes ($C = 15$ in Intent-QA), 2 corresponds to the object or part prediction of each class, and 1 is for the background class. The output is supervised only on the annotated points using cross-entropy loss. In Sec. 6 we show that this model produces comparable results to the Local-QA-model.

Global-QA-model. Finally, we adapt the Local-QA-model to the LookTwice-QA setting, producing a Global-QA-model that combines local with global contextual reasoning. Let $f(\mathbf{v}_i, \mathbf{q})$ be the function used to compute the attention a_i over region i in step (e); this function projects the inputs to a common space, multiplies them element-wise and runs through fully-connected layers to produce an attention score. Assume f is then normalized to a probability distribution over the N regions. Let $g(\mathbf{q}, \mathbf{v})$ be the function used to compute the distribution over the final answers in step (g) by projecting the inputs to a common vector space, then computing element-wise multiplication followed by fully connected layers and sigmoid outputs.

The Global-QA-model is $g(\mathbf{q}, \mathbf{v}^{pt}, \mathbf{v}^{all})$, where the probability distribution over the final answers is computed considering both a local \mathbf{v}^{pt} and global \mathbf{v}^{all} visual features. We define $\mathbf{v}^{pt} = \sum_i f(\mathbf{v}_i^{pt}, \mathbf{q}) \mathbf{v}_i^{pt}$, i.e., identically to the Local-QA-model as the attention-weighted sum of the visual features \mathbf{v}_i^{pt} of the N regions; recall that the regions in the Local-QA-model were constrained to contain the input point (x, y) in step (a) prior to non-maximum suppression. The global features are computed as $\mathbf{v}^{all} = \sum_i f(\mathbf{v}_i^{all}, \mathbf{v}^{pt}, \mathbf{q}) \mathbf{v}_i^{all}$, i.e., a weighted sum over the visual features \mathbf{v}_i^{all} corresponding to the set of N image regions from step (c) in the standard VQA models, without any filtering to include the input point (x, y) . Here the attention f depends on the region features \mathbf{v}_i^{all} , the question \mathbf{q} but also the local representation \mathbf{v}^{pt} . The intuition is that \mathbf{v}^{pt} extracts local information relevant to the question, which is then used to attend to other relevant image regions.

6. Experimental results

We implemented the models of Sec. 5 and benchmarked them on the datasets of Sec. 4. We focus primarily on the analysis of the findings to gain insights into the new tasks.

6.1. Local-QA results

Implementation details. We benchmark Local-QA-model and Local-QA-grid-model trained on *train* of Local-QA. For both models we build off the state-of-the-art Pythia model [32] for steps (d)-(g) above (visual attention + prediction). For Local-QA-model, we use a Feature Pyramid Network (FPN) [20] to compute region features and IOU of 0.5 for non-maximum suppression, as in the VQA Chal-

lenge implementation of Pythia. For Local-QA-grid-model we compute grid features using the modified Faster-RCNN in [18]. For fair comparison, a ResNet-101 [14] backbone is used for both models. All models were trained using the AdaMax optimizer with a learning rate of 0.002. We use early stopping on the *val* set with patience of 500 iterations.

Test accuracy and ablations. The Local-QA-model achieves 76.6% accuracy on *test-final* compared to only 65.9% of Local-QA-grid-model. Table 1 reports results on *test-dev* where we experiment with several different methods for incorporating a point input across both models. For region features, our strategy in Local-QA-model of removing regions not containing the point and allowing the model to learn attention over the rest achieves at least 5.8% improvement over simpler strategies such as removing all but the smallest or the highest-scoring region proposal containing the point. Improvement is particularly significant on action questions, where other methods perform 12.6% worse.

Region vs grid features. There is a significant difference in accuracy between our models for region (75.0%) and grid features (64.0%). Notably, our Local-QA-model *benefits* from learning attention over region proposals containing the point, while our Local-QA-grid-model restricts its view of the grid to only a single downsampled point location. The superior performance of region features can be explained by the fact that region proposals at different scales are already provided around the point; for grid features, it is less clear how to restrict the model’s view of the grid using the point, and any approach risks providing too little relevant information or too much irrelevant information. Thus, we focus on the Local-QA-model framework going forward.

Attention analysis. An average of 27 region proposals containing the point are provided as input to our Local-QA-model. The model’s probabilistic attention is relatively peaked, with the maximum attention of 0.548 on average in *test-dev*. The size of the maximum attention region is only 71% the size of the ground-truth object bounding box on average, likely because smaller bounding boxes are sufficient to infer attributes such as color and action. An important property is the model’s ability to attend based on the question. For the 799 questions in *test-dev* that ask “What color is this shirt?”, we can change the question to “What action is this person doing?”. This increases the median size of the max-attention region from 2,997 to 5,451 pixels, indicating that the model shifts its attention accordingly (Fig. 5).

6.1.1 Spatial vs Verbal Disambiguation

For many local-QA questions, a disambiguating phrase could be provided as a substitute for a point (e.g. “What color is the car *on the left*?”) Such verbal disambiguation is often unnatural and can quickly grow expensive depending on the object of interest; this partially explains why humans

	Strategy	QIPBA	Overall	Color	Action	Shape
Priors	Q-only	+ - - - -	27.8	25.8	45.5	32.1
	Modal-A	- - - - +	52.2	52.0	60.1	52.8
Grid	Full Img	+ + - - -	35.7	35.4	45.5	35.9
	Top-score	+ + + - -	50.8	51.0	45.5	35.9
	Smallest	+ + + - -	63.6	64.4	45.5	32.1
	Ours	+ + + - -	64.0	64.4	58.0	37.7
	GT box	+ + - - -	80.2	80.7	67.1	60.4
Region	Full Img	+ + - - -	37.4	37.2	45.4	35.9
	Top-score	+ + + - -	44.8	44.4	62.2	43.4
	Smallest	+ + + - -	69.2	69.6	58.0	56.6
	Ours	+ + + - -	75.0	75.4	66.4	56.6
	GT box	+ + - - -	80.2	80.7	67.1	60.4

Table 1. Accuracy (in %) of different models and baselines on the Local-QA *test-dev* split. The QIPBA column indicates the model input: Question, Image, Point, ground truth Bounding box, and/or the set of all correct Answers in the image. Modal-A is a baseline oracle that selects the mode answer among all answers that are *correct* in this image; Grid is the Local-QA-grid-model; Region is Local-QA-model. Strategies: Q-only relies only on dataset language priors; Full Img is the original model of [18] for Grid and Pythia [32] for Region, not consuming the point input; Top-score and Smallest take the features of only the highest-scoring or smallest region proposal containing the point respectively (downsampling for grid features, restricting the attention to a single region for region features). Our proposed models outperform these alternatives, and the Region-based Local-QA-model even performs close to the accuracy that is achieved when the ground truth box instead of the point is provided during training and testing.

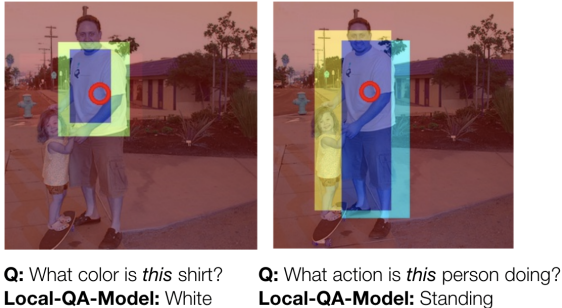


Figure 5. Local-QA-model successfully varies attention around the point in response to a question. (Darker = higher attention). Point is indicated in red.

prefer to point, and motivates pointing as a more natural and realistic setup for a broad set of visual questions. However, we briefly provide a comparison between verbal and spatial disambiguation.

Data. We collect a small dataset using human-written questions from Visual Genome [19]. A parser is used to detect the question subject, and we (1) ensure this object appears multiple times in the image and (2) search for prepositional phrases appended to the question subject to detect verbal disambiguation. Using object/attribute annotations, the question’s subject is matched to an object in the image,



Figure 6. In both examples, the standard verbal-only VQA model (top) fails to understand the verbal disambiguation and picks an answer corresponding to the wrong object instance; the Local-QA-model (bottom) correctly incorporates the point input.

and a “spatial version” of the question is generated by removing verbal disambiguation from the question and generating a point from the center of the target object’s bounding box. We thus generate a verbally disambiguating version of the dataset D_V and a spatial disambiguating version D_S , with 1,855 questions across 1,575 images in each. We use 80% for training and 10% each for validation and testing.

Results. Our Local-QA-model leveraging the point input achieves an accuracy of 66.5% on D_S , while the Pythia [32] baseline relying on verbal disambiguation achieves only 26.5% on D_V (Fig. 6). Note that a question-only model gets 22.2% accuracy on D_V ; thus, the baseline does not effectively understand verbal disambiguation. This further motivates point-input questions as an extension of VQA.

6.2. Intent-QA results

Implementation details. We benchmark Local-QA-model and Local-Segm-model trained on *train* of Intent-QA. Local-QA-model is trained as in Sec. 6.1 with one exception: since the model may need to focus on object parts in addition to whole objects, we use all proposed regions rather than running non-maximum suppression. (On *test-dev*, the accuracy is 75.0% with nms and 77.1% without). The Local-Segm-model uses the ResNet-101 backbone [14] pretrained on ImageNet. It is trained using the Adam optimizer with a fixed learning rate of $2.4e-4$.

Adapting Local-QA-model to the task. The Intent-QA task requires the model to infer whether each point is referring to the full object or just a part of the object. Table 2 evaluates variations of the Local-QA-model; the key finding is that directly training the model to produce the answer “full object” or “object part” appears superior to providing additional object class information in the question. Going forward, we ask “What is *this* referring to?” and expect an “object” or “part” answer.

Local-QA-model vs Local-Segm-model. Results on *test-final* comparing Local-QA-model to Local-Segm-model are in Table 3. Local-QA-model achieves 77.4% accuracy, slightly behind Local-Segm-model at 77.9%.¹ A simple

¹Local-Segm-model achieves 61.2% accuracy on its 31-way predictions; we convert the predictions to binary using Method (1) in Table 2.

Question	Answers	Inf.	Accuracy
Is this referring to a part?	yes/no	-	59.7
Is <i>this</i> referring to a part?	yes/no	-	77.2
What is <i>this</i> referring to?	object/part	-	77.2
Is <i>this</i> [object class] point referring to a part?	yes/no	-	77.1
		(1)	75.6
What is <i>this</i> referring to?	30 classes	(2)	75.2
		(3)	57.5

Table 2. Evaluating variations of the Local-QA-model on *test-dev* of Intent-QA (accuracy in %). The first row is the baseline accuracy of asking the question without the point input, which reflects dataset priors. The next two rows verify that as expected the question formulation or the semantic meaning of the two answers has no impact on accuracy here since the same question is asked across all images and only the point input varies. Somewhat surprisingly, the next row shows that even including the object class in the question has little bearing on accuracy. The last three rows increases the set of answers to 30 during training (15 object classes, with 2 possible answers for each, e.g., “cat part” or “entire cat”). For completeness, the test-time 30-way accuracy is 70.9%. The three different test-time inference (Inf.) strategies to convert to the binary outputs are: (1) condition on the correct object class and take the highest of the two part-or-object probabilities, (2) take the single highest answer and report whether it corresponds to the full object or part, regardless of the predicted object class, and (3) marginalize over the object classes by summing the 15 probabilities corresponding to full objects and the 15 probabilities. Directly training the binary answers achieves the highest accuracy despite the extra training-time supervision provided to the 30-way model.

Method	Overall	Obj	Part	Amb	Not
Local-QA-model	77.4	74.3	79.7	67.8	81.8
Local-Segm-model	77.9	78.8	77.3	65.9	84.1

Table 3. Accuracy (in %) on Intent-QA *test-final*. “Amb” refers to ambiguous points (human annotations contain disagreement).

baseline that predicts the more common answer (“part”) yields an accuracy of only 57.2%, validating that both models are able to effectively reason about human intention. Average human annotator accuracy (evaluated against the other annotators) is 86.9%. As expected, both models achieve significantly higher accuracy on unambiguous points (where all human annotators agree) than on ambiguous points: e.g., 67.8% on ambiguous vs 81.8% on unambiguous for Local-QA-model.

Model analysis. The Local-QA-model allows us to evaluate the learned attention by looking at the statistics of the highest-attention region on points referring to a full object (5,911 pixels on average, 0.15 IOU with the object bounding box) versus points referring to an object part (much smaller, 4,092 pixels on average, but arguably better localized, with 0.31 IOU with the part bounding box). Fig. 7

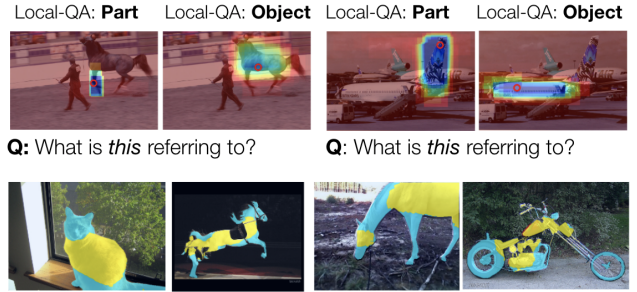


Figure 7. (Top) Local-QA-model shifts attention for part vs object points. Point is indicated in red. (Bottom) Local-Segm-model’s predictions at every pixel on the object; blue = object part, yellow = whole object.

	Spatial Disambiguation			Prior
	None	Point	Box	
How many of <i>these</i> ...	39.6	49.6	52.3	35.4
How many of <i>these</i> [supercategory]...	44.7	51.1	51.7	36.3
How many [object]...	52.6	52.2	52.4	42.1

Table 4. Results of Global-QA-model on the LookTwice-QA *test*. Rows are the question asked; columns are the level of spatial disambiguation provided. Prior is a language-only model.

(top) demonstrates this visually. For Local-Segm-model we explicitly evaluate the predictions at every pixel as shown Fig. 7 (bottom), demonstrating that the model is able to reason in sophisticated ways about object/part inference. While distance from object center is a useful cue, a simple baseline based only on centroid distance achieves an accuracy of only 61.1% (vs 77.9% of Local-Segm-model).

6.3. LookTwice-QA results

We benchmark the Global-QA-model trained on LookTwice-QA; implementation details as in Sec. 6.1.

Test accuracy. When trained to answer the question “How many of *these* are there?” along with a disambiguating point input, the Global-QA-model achieves an accuracy of 49.6%, significantly higher than an image-only version (without the point) at 39.6% and the modal answer (“1”) baseline at 35.4%, and as expected somewhat behind having access to the bounding box at 52.3%. In Table 4 we demonstrate how the accuracy changes with decreasing the ambiguity of the question: specifying the supercategory (being, vehicle or object) boosts the accuracy from 49.6% to 51.1%, and naming the object class further boosts it to 52.2% (making the need for spatial supervision irrelevant, as the image-only model achieves 52.6% in this setting).

Attention analysis. We consider the Global-QA-model trained on supercategory questions. There are two types of attention: local attention around the point is relatively peaked, with an average max attention of 0.42; as expected,



Figure 8. Attention of the Global-QA-model on a question in the LookTwice-QA test set. Point is indicated in red.

global attention on the image is diffuse with an average max attention of 0.07. An example result is shown in Fig. 8.

Global-QA-model vs Local-QA-model. Finally, we demonstrate the need for the Global-QA-model architecture by comparing with Local-QA-model which only considers regions overlapping the point. The Local-QA-model achieves an accuracy of 46.8% on super-category questions, significantly lower than Global-QA-model at 51.1%. As expected, this is due to under-counting by Local-QA-model. Concretely, on questions with the answer “1,” Local-QA-model actually performs better (75.8% vs. 68.6% of Global-QA-model); however, for answer ≥ 2 , Global-QA-model achieves 41.9% and Local-QA-model only 31.9%.

Conclusions. In summary, we introduced three novel types of visual questions *requiring* a spatial point input for disambiguation. For each question type we created a benchmark dataset and a baseline model and performed extensive analysis. We hope that our work inspires further research in this space of questions.

Acknowledgments. This work is partially supported by Samsung and by the Princeton SEAS Project-X Funding Award. Thank you to Karthik Narasimhan, Zeyu Wang, Felix Yu, Zhiwei Deng, and Deniz Oktay for helpful discussions and feedback on this work.

References

- [1] Aishwarya Agrawal, Dhruv Batra, Devi Parikh, and Aniruddha Kembhavi. Don’t Just Assume; Look and Answer: Overcoming Priors for Visual Question Answering. In *Conference on Computer Vision and Pattern Recognition*, 2018. 2
- [2] Peter Anderson, Xiaodong He, Chris Buehler, Damien Teney, Mark Johnson, Stephen Gould, and Lei Zhang. Bottom-up and top-down attention for image captioning and visual question answering. In *IEEE Conference on Computer Vision and Pattern Recognition (CVPR)*, 2018. 2, 5
- [3] Stanislaw Antol, Aishwarya Agrawal, Jiasen Lu, Margaret Mitchell, Dhruv Batra, C. Lawrence Zitnick, and Devi Parikh. VQA: Visual Question Answering. In *International Conference on Computer Vision (ICCV)*, 2015. 1
- [4] Amy Bearman, Olga Russakovsky, Vittorio Ferrari, and Li Fei-Fei. What’s the point: Semantic segmentation with point supervision. In *European Conference on Computer Vision (ECCV)*, 2016. 2
- [5] Sean Bell, Paul Upchurch, Noah Snavely, and Kavita Bala. Material recognition in the wild with the materials in context database. 2015. 2
- [6] Xianjie Chen, Roozbeh Mottaghi, Xiaobai Liu, Sanja Fidler, Raquel Urtasun, and Alan Yuille. Detect what you can: Detecting and representing objects using holistic models and body parts. In *Conference on Computer Vision and Pattern Recognition (CVPR)*, 2014. 3, 4
- [7] Abhishek Das, Samyak Datta, Georgia Gkioxari, Stefan Lee, Devi Parikh, and Dhruv Batra. Embodied Question Answering. In *Conference on Computer Vision and Pattern Recognition (CVPR)*, 2018. 1, 2
- [8] Abhishek Das, Satwik Kottur, Khushi Gupta, Avi Singh, Deshraj Yadav, Jose M. F. Moura, Devi Parikh, and Dhruv Batra. Visual dialog. In *Conference on Computer Vision and Pattern Recognition (CVPR)*, 2017. 1
- [9] Mark Everingham, Luc Van Gool, Christopher K. I. Williams, John Winn, and Andrew Zisserman. The Pascal Visual Object Classes (VOC) challenge. 2010. 3, 4
- [10] Chaz Firestone and Brian J. Scholl. Please Tap the Shape, Anywhere You Like: Shape skeletons in human vision revealed by an exceedingly simple measure. *Psychological Science*, 25(2):377–386, 2014. 4
- [11] Chuang Gan, Yandong Li, Haoxiang Li, Chen Sun, and Boqing Gong. VQS: Linking Segmentations to Questions and Answers for Supervised Attention in VQA and Question-Focused Semantic Segmentation. In *International Conference on Computer Vision (ICCV)*, 2017. 2
- [12] Daniel Gordon, Aniruddha Kembhavi, Mohammad Rastegari, Joseph Redmon, Dieter Fox, and Ali Farhadi. Iqa: Visual question answering in interactive environments. In *Proceedings of the IEEE Conference on Computer Vision and Pattern Recognition (CVPR)*, 2018. 2
- [13] Yash Goyal, Tejas Khot, Aishwarya Agrawal, Douglas Summers-Stay, Dhruv Batra, and Devi Parikh. Making the V in VQA Matter: Elevating the Role of Image Understanding in Visual Question Answering. 2019. 1, 2
- [14] Kaiming He, Xiangyu Zhang, Shaoqing Ren, and Jian Sun. Deep residual learning for image recognition. In *Conference on Computer Vision and Pattern Recognition (CVPR)*, 2016. 6, 7
- [15] Michael Hild, Motonobu Hashimoto, and Kazunobu Yoshida. Object recognition via recognition of finger pointing actions. In *Image Analysis and Processing*, 2003. 2
- [16] Drew A. Hudson and Christopher D. Manning. GQA: A New Dataset for Real-World Visual Reasoning and Compositional Question Answering. In *Conference on Computer Vision and Pattern Recognition (CVPR)*, 2019. 1, 2
- [17] Suyog Dutt Jain and Kristen Grauman. Click carving: Segmenting objects in video with point clicks. In *AAAI Conference on Human Computation and Crowdsourcing (HCOMP)*, 2016. 2

- [18] Huaizu Jiang, Ishan Misra, Marcus Rohrbach, Erik Learned-Miller, and Xinlei Chen. In defense of grid features for visual question answering. In *IEEE Conference on Computer Vision and Pattern Recognition (CVPR)*, 2020. 5, 6, 7
- [19] Ranjay Krishna, Yuke Zhu, Oliver Groth, Justin Johnson, Kenji Hata, Joshua Kravitz, Stephanie Chen, Yannis Kalantidis, Li-Jia Li, David A. Shamma, Michael S. Bernstein, and Li Fei-Fei. Visual Genome: Connecting Language and Vision Using Crowdsourced Dense Image Annotations. In *International Journal of Computer Vision*, 2017. 1, 2, 3, 4, 7
- [20] Tsung-Yi Lin, Piotr Dollár, Ross B. Girshick, Kaiming He, Bharath Hariharan, and Serge J. Belongie. Feature pyramid networks for object detection. *2017 IEEE Conference on Computer Vision and Pattern Recognition (CVPR)*, pages 936–944, 2017. 6
- [21] Jonathan Long, Evan Shelhamer, and Trevor Darrell. Fully convolutional networks for semantic segmentation. In *Conference on Computer Vision and Pattern Recognition (CVPR)*, 2015. 6
- [22] Bertram F Malle, Louis J Moses, and Dare A Baldwin. *Intentions and intentionality: Foundations of social cognition*. MIT press, 2001. 1, 2
- [23] David Merrill and Pattie Maes. Augmenting looking, pointing and reaching gestures to enhance the searching and browsing of physical objects. In *Pervasive Computing*. 2007. 2
- [24] Roozbeh Mottaghi, Xianjie Chen, Xiaobai Liu, Nam-Gyu Cho, Seong-Whan Lee, Sanja Fidler, Raquel Urtasun, and Alan Yuille. The role of context for object detection and semantic segmentation in the wild. In *Conference on Computer Vision and Pattern Recognition (CVPR)*, 2014. 4
- [25] John Oates and Andrew Grayson. *Cognitive and language development in children*. Blackwell; Open University Press, 2004. 1, 2
- [26] Dim P. Papadopoulos, Alasdair D. F. Clarke, Frank Keller, and Vittorio Ferrari. Training object class detectors from eye tracking data. In *European Conference of Computer Vision (ECCV)*, 2014. 2
- [27] Dong Huk Park, Lisa Anne Hendricks, Zeynep Akata, Anna Rohrbach, Bernt Schiele, Trevor Darrell, and Marcus Rohrbach. Multimodal Explanations: Justifying Decisions and Pointing to the Evidence. In *Conference on Computer Vision and Pattern Recognition (CVPR)*, 2018. 2
- [28] Syed Shaikat Raza Abidi, MaryAnn Williams, and Benjamin Johnston. Human pointing as a robot directive. In *International Conference on Human-robot interaction*, 2013. 2
- [29] Shaoqing Ren, Kaiming He, Ross B. Girshick, and J. Sun. Faster r-cnn: Towards real-time object detection with region proposal networks. *IEEE Transactions on Pattern Analysis and Machine Intelligence*, 39:1137–1149, 2015. 5
- [30] Allison Sauppe and Bilge Mutlu. Robot deictics: how gesture and context shape referential communication. In *International Conference on Human-Robot Interaction*, 2014. 2
- [31] Zhou Yu, Jun Yu, Yuhao Cui, Dacheng Tao, and Qi Tian. Deep modular co-attention networks for visual question answering. In *Proceedings of the IEEE Conference on Computer Vision and Pattern Recognition (CVPR)*, 2019. 2, 5
- [32] Yu Jiang*, Vivek Natarajan*, Xinlei Chen*, Marcus Rohrbach, Dhruv Batra, and Devi Parikh. Pythia v0.1: the winning entry to the vqa challenge 2018. 2018. 2, 5, 6, 7
- [33] Yundong Zhang, Juan Carlos Nieves, and Alvaro Soto. Interpretable Visual Question Answering by Visual Grounding From Attention Supervision Mining. In *IEEE Winter Conference on Applications of Computer Vision (WACV)*, 2019. 2
- [34] Yuke Zhu, Oliver Groth, Michael Bernstein, and Li Fei-Fei. Visual7w: Grounded Question Answering in Images. In *Conference on Computer Vision and Pattern Recognition (CVPR)*, 2016. 1, 2